applied optics

Development and accuracy of a multipoint method for measuring visibility

Hongda Tai,[1,2] Zibo Zhuang,[2] and Dongsong Sun[1,*]

[1]School of Earth and Space Sciences, University of Science and Technology of China, Jinzhai Road No.96, Hefei 230026, China
[2]Aeronautical Meteorology Department, College of Air Traffic Management, Civil Aviation University of China, Tianjin 300300, China
*Corresponding author: sds@ustc.edu.cn

Received 19 July 2017; revised 3 September 2017; accepted 5 September 2017; posted 7 September 2017 (Doc. ID 302497); published 28 September 2017

Accurate measurements of visibility are of great importance in many fields. This paper reports a multipoint visibility measurement (MVM) method to measure and calculate the atmospheric transmittance, extinction coefficient, and meteorological optical range (MOR). The relative errors of atmospheric transmittance and MOR measured by the MVM method and traditional transmissometer method are analyzed and compared. Experiments were conducted indoors, and the data were simultaneously processed. The results revealed that the MVM can effectively improve the accuracy under different visibility conditions. The greatest improvement of accuracy was 27%. The MVM can be used to calibrate and evaluate visibility meters.

OCIS codes: (010.1290) Atmospheric optics; (010.1320) Atmospheric transmittance; (010.7295) Visibility and imaging.

https://doi.org/10.1364/AO.56.007952

1. INTRODUCTION

Visibility is an important element of meteorological observations. The need for accurate real-time visibility information is increasing for many applications, such as highway closures, vehicle speed limits, aircraft takeoff and landing, air quality monitoring, and military activities [1]. Low-visibility weather events, such as haze and dust storms, which are becoming more frequent in China [2] and in many parts of the world [3], not only degrade the air quality and threaten human health but also lead to severe traffic accidents.

For meteorological purposes, visibility was first defined as a quantity to be estimated by a human observer. The weather, sun angle, light intensity, darkness adaptation, availability of appropriate visibility targets, and individual physical abilities determine the quality of a person's perception of atmospheric conditions [4]. The meteorological optical range (MOR) can be measured objectively, and it represents the transparency of the atmosphere. Large numbers of visibility sensors based on several different measuring principles are now commonly used to automatically measure the MOR.

The two main types of visibility sensors are transmissometers and forward scatter sensors [5]. Engel and Heyn [6], Wayne and Reinhardt [7], Mohan *et al.* [8], Chandran *et al.* [9], and Kaurila [10] designed and applied transmissometers to measure visibility. Barrales-Guadarrama *et al.* [11], Kähkönen *et al.* [12], and Siikamaki [13] described forward scatter visibility sensors. Wang *et al.* [1], Tang *et al.* [14], Caimi *et al.* [15], and Babari *et al.* [16] used cameras to measure visibility. Czarnecki *et al.* [4] and Taillade *et al.* [17] reported visibility sensors based on the relationship between atmospheric visibility and Light Detection and Ranging (LiDAR) backscatter signals.

Many studies have evaluated the performance of visibility sensors by comparing different types of sensors. The results measured by transmissometers are often utilized as standards in these comparison studies. For example, Griggs *et al.* [18] reported the results of the first World Meteorological Organization (WMO) comparison of visibility measurements in which the data collected by 14 transmissometers, 10 forward scatter visibility meters, and one backward scatter visibility sensor over a seven-month period in the United Kingdom were compared. Waas [19] conducted a field test at three international airports using 11 forward scatter sensors operated in parallel to the existing transmissometers to gain operational experience with forward sensors and to decide which type of visibility sensor should be acquired. Bloemink [20] compared transmissometers and forward scatter sensors over a 12-month period and reported the Koninklijk Nederlands Meteorologisch Instituut (Royal Netherlands Meteorological Institute [KNMI]) visibility standard for the calibration of scatter meters. Chan [21] conducted a field study of visibility sensors at the meteorological garden of the Hong Kong International Airport. The work highlights the importance

of testing the performance of visibility sensors in the context of the various types of weather that affect a particular place or region, especially those associated with haze conditions.

Since transmissometers measure the loss of light from a collimated beam as a result of molecular and aerosol scattering and absorption, their operational principals are closely related to the definition of MOR. A high-quality, well-maintained transmissometer working at maximum accuracy provides a very good approximation of the true MOR [5]. However, the transmissometer system was sensitive to window contamination, and it required extensive window cleaning. Meanwhile, the single baseline could not cover the full visibility dynamic range, and the short baseline had large forward scatter errors and was difficult to align [22]. Crosby [23] examined several key areas to define the accuracy of visibility sensors and noted that the sensor consistency with a transmissometer, which is reported in many comparisons, is a useful parameter but is not a substitute for the ability of a sensor to take accurate measurements in real-world conditions. Thus, reducing the measurement error of visibility sensors and improving the accuracy of visibility measurements are important goals.

This paper proposes a new method for visibility measurements with a measurement error that is much smaller than that of transmissometers, as evidenced by an error analysis. This experimental system is capable of providing visibility measurements with improved accuracy.

2. METHOD

A. Measurement of Atmospheric Transmittance

The multipoint visibility measurement (MVM) system is composed of a fixed transmitter module and a mobile receiver module. The mobile receiver stops every 5 m and collects measurements at a total of n points. $P_1(0) \sim P_n(0)$ represent the laser power when the mobile receiver stops because of the unavoidable power instability of the laser device. $P_r(1) \sim P_r(n)$ represent the power received at different stops, as depicted in Fig. 1.

First, the mobile receiver is moved to position 0. At this point, the laser transmits directly into the receiver without passing through the atmosphere. The attenuation of the laser power T_0 caused by the lens, photodetector, and data-acquisition card can be described as

$$T_0 = P(0) - P_r(0), \tag{1}$$

where $P(0)$ is the laser power of the time, and $P_r(0)$ is the power received at position 0.

When the mobile receiver moves to position 1 (i.e., 5 m), the power of the transmitter of the time is $P_1(0)$ because of the unavoidable power instability. The attenuation of the laser power T_1 of the time is described as

$$T_1 = P_1(0) - P_r(1), \tag{2}$$

where T_1 is the total laser power attenuation of the system, including both the light attenuation attributable to the 5 m of atmosphere in the laser beam's path (T_1') and that caused by the system components, such as the lens, photodetector, and data-acquisition card, which are closely related to the laser power of the time. This value changes from when the mobile receiver stops at position 0 to $\frac{P_1(0)}{P(0)} T_0$ when the mobile receiver stops at position 1, as follows:

$$T_1 = T_1' + \frac{P_1(0)}{P(0)} T_0. \tag{3}$$

As a result, to eliminate the optical attenuation of the system itself, the accurate laser power preparing to transmit into the atmospheric can be regarded as $P_1(0) - \frac{P_1(0)}{P(0)} T_0$. The accurate value of the atmospheric transmittance when the mobile receiver stops at position 1 can be calculated as follows:

$$\tau(r_1) = \frac{P_r(1)}{P_1(0) - \frac{P_1(0)}{P(0)} T_0} = \frac{P(0) \cdot P_r(1)}{P(0) \cdot P_1(0) - P_1(0) \cdot T_0}. \tag{4}$$

Substituting T_0 into Eq. (4) using Eq. (1),

$$\tau(r_1) = \frac{P(0) \cdot P_r(1)}{P_1(0) \cdot P_r(0)}. \tag{5}$$

The atmospheric transparency can be assumed to remain constant during the experiment; therefore, the atmospheric transmittance measured at point N can be described as

$$\tau(r_n) = \frac{P(0) \cdot P_r(n)}{P_n(0) \cdot P_r(0)}, \tag{6}$$

where $P_n(0)$ is the laser power when the mobile receiver stops at measurement point N, and $P_r(n)$ is the power received by the mobile receiver at measurement point N. A set of atmospheric transmittance values (i.e., N values) can be obtained using Eq. (6).

B. Calculation of Extinction Coefficients

According to the Beer–Lambert law, the relationship between the atmospheric transmittance and the extinction coefficient is

$$\ln \tau(r_n) = -\delta \cdot r_n \qquad (n = 1, 2, 3, \ldots, n), \tag{7}$$

where $\tau(r_n)$ represents the atmospheric transmittance values when the mobile receiver stops at several fixed points, and the baselines between the laser source and the mobile receiver are r_n.

In the coordinate system where r_n is the x axis and $\ln \tau(r_n)$ is the y axis, the slope of the straight line, which can be obtained by the least squares method, is simply the inverse of the extinction coefficient, as depicted in Fig. 2.

Since the least squares method can produce the minimum sum of the squared residuals, the extinction coefficients can be obtained as follows:

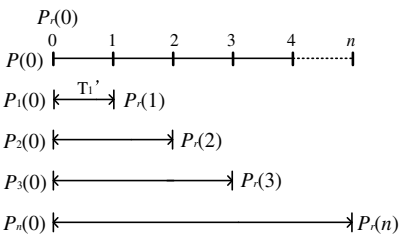

Fig. 1. Schematic diagram of the MVM system.

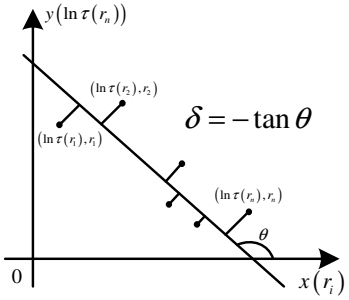

Fig. 2. Extinction coefficient obtained by the least squares method.

$$\sum_{i=1}^{n}[\ln \tau(r_i) - (-\delta \cdot r_i)]^2 = \sum_{i=1}^{n}[\ln \tau(r_i) + \delta \cdot r_i]^2 = \text{Min}. \tag{8}$$

Because the second derivative of Eq. (8) is always greater than 0, the extinction coefficients can be obtained from the first derivative of Eq. (8), that is,

$$\delta = -\frac{\sum_{i=1}^{n} r_i \cdot \ln \tau(r_i)}{\sum_{i=1}^{n} r_i^2}. \tag{9}$$

In Eq. (9), $r_i = 5$ m, 10 m, 15 m, 20 m, 25 m, 30 m, 35 m, 40 m, 45 m, and 50 m. Substituting $\tau(r_i)$ in Eq. (9) using Eq. (6) allows the extinction coefficients to be measured.

C. Calculation of the MOR

According to Koschmieder's law, the MOR can be calculated as

$$\text{MOR} = \frac{-\ln \varepsilon}{\delta}, \tag{10}$$

where ε is the visual threshold of human eyes, typically 0.05 according to WMO and International Civil Aviation Organization (ICAO) regulations. Therefore, Eq. (10) can be rewritten as follows:

$$\text{MOR} = -\frac{\ln 0.05}{\delta} \approx \frac{3}{\delta}. \tag{11}$$

Substitute Eq. (9) into Eq. (11) to obtain Eq. (12), as follows:

$$\text{MOR} = -\frac{3 \cdot \sum_{i=1}^{n} r_i^2}{\sum_{i=1}^{n} r_i \cdot \ln \tau(r_i)}. \tag{12}$$

3. ERROR ANALYSIS

A. Relative Error of Atmospheric Transmittance

1. Relative Error of the Transmissometer

As mentioned above, the results measured by transmissometers are often utilized as standards in comparison studies. The atmospheric transmittance of a traditional transmissometer can be described as

$$\tau = \frac{P_d(r)}{P_d(0)}, \tag{13}$$

where $P_d(0)$ is the power emitted from the transmitter, and $P_d(r)$ is the power received by the receiver, as shown in Fig. 3.

The system error for atmospheric transmittance of the transmissometer is

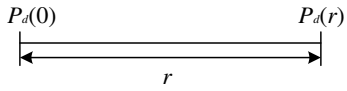

Fig. 3. Schematic of a transmissometer.

$$\Delta\tau = \frac{1}{P_d(0)} \cdot \Delta P_d(r) + \frac{-P_d(r)}{[P_d(0)]^2}\Delta P_d(0) \tag{14}$$

and the relative error for atmospheric transmittance is as follows:

$$\frac{\Delta\tau}{\tau} = \frac{\Delta P_d(r) + \frac{-P_d(r)}{P_d(0)}\Delta P_d(0)}{P_d(r)} = \frac{\Delta P_d(r)}{P_d(r)} - \frac{\Delta P_d(0)}{P_d(0)}. \tag{15}$$

Equation (15) shows that the atmospheric transmittance relative error of the transmissometer is the difference of the relative system error between the transmitter and receiver. To facilitate the back calculation, we assume that the result of Eq. (15) is n%, that is:

$$\frac{\Delta\tau}{\tau} = \frac{\Delta P_d(r)}{P_d(r)} - \frac{\Delta P_d(0)}{P_d(0)} = n\%. \tag{16}$$

2. Relative Error of the MVM System

Equation (6) shows that the atmospheric transmittance system error of the MVM system (MVMS) is as follows:

$$\begin{aligned}\Delta\tau(r_n) = {} & \frac{P_r(n)}{P_n(0)\cdot P_r(0)}\Delta P(0) + \frac{P(0)}{P_n(0)\cdot P_r(0)}\Delta P_r(n) \\ & + \frac{-P(0)\cdot P_r(n)}{P_r(0)\cdot [P_n(0)]^2}\Delta P_n(0) + \frac{-P(0)\cdot P_r(n)}{P_n(0)\cdot [P_r(0)]^2}\Delta P_r(0).\end{aligned} \tag{17}$$

The relative error of the atmospheric transmittance of the MVMS can be calculated using Eqs. (6) and (17), as follows:

$$\begin{aligned}\frac{\Delta\tau(r_n)}{\tau(r_n)} &= \frac{\frac{P_r(n)}{P_n(0)\cdot P_r(0)}\Delta P(0) + \frac{P(0)}{P_n(0)\cdot P_r(0)}\Delta P_r(n) + \frac{-P(0)\cdot P_r(n)}{P_r(0)\cdot [P_n(0)]^2}\Delta P_n(0) + \frac{-P(0)\cdot P_r(n)}{P_n(0)\cdot [P_r(0)]^2}\Delta P_r(0)}{\frac{P(0)\cdot P_r(n)}{P_n(0)\cdot P_r(0)}} \\ &= \left[\frac{\Delta P_r(n)}{P_r(n)} - \frac{\Delta P_r(0)}{P_r(0)}\right] - \left[\frac{\Delta P_n(0)}{P_n(0)} - \frac{\Delta P(0)}{P(0)}\right].\end{aligned} \tag{18}$$

For atmospheric transmittance, the difference in the relative error between the MVMS and the transmissometer can be described using Eqs. (15) and (18) as follows:

$$\begin{aligned}&\frac{\Delta\tau_d}{\tau_d} - \frac{\Delta\tau(r_n)}{\tau(r_n)} \\ &= \frac{\Delta P_d(r)}{P_d(r)} - \frac{\Delta P_d(0)}{P_d(0)} \\ &\quad - \left[\left(\frac{\Delta P_r(n)}{P_r(n)} - \frac{\Delta P_r(0)}{P_r(0)}\right) - \left(\frac{\Delta P_n(0)}{P_n(0)} - \frac{\Delta P(0)}{P(0)}\right)\right].\end{aligned} \tag{19}$$

If the baseline length of the MVMS and the transmissometer is the same when the MVMS receiver is moved to measurement point N, then at this time, equations

$$P_n(0) = P_d(0), \tag{20}$$

$$P_r(n) = P_d(r), \tag{21}$$

can be expressed, where $P_n(0)$ and $P_r(n)$ are the transmitter and receiver power of the MVMS, and $P_d(0)$ and $P_d(r)$ are the transmitter and receiver power of the transmissometer, respectively.

Substitute Eqs. (20) and (21) into Eq. (19) to obtain the following:

$$\frac{\Delta\tau_d}{\tau_d} - \frac{\Delta\tau(r_n)}{\tau(r_n)} = \frac{\Delta P_r(0)}{P_r(0)} - \frac{\Delta P(0)}{P(0)}. \tag{22}$$

For atmospheric transmittance, the difference in the relative error between the transmissometer and the MVMS is simply the difference in the relative error between the MVMS transmitter and receiver for power when the baseline length is 0.

Equation (3) shows that when the baseline is r, the total light attenuation of the MVMS can be described as

$$T_r = P_n(0) - P_r(n) = T_r' + \frac{P_n(0)}{P(0)} T_0, \tag{23}$$

where T_r' is the atmospheric light attenuation with a baseline length of r, and the light attenuation caused by the MVMS itself is $\frac{P_n(0)}{P(0)} T_0$.

According to Eqs. (7) and (11), if the visibility and baseline length are known, then the true value of atmospheric transmittance can be calculated.

If the true value of atmospheric transmittance at this time is τ_0, then

$$T_r' = (1 - \tau_0) P_n(0). \tag{24}$$

If the atmospheric transmittance measured by the transmissometer with a baseline length of r is τ_d, and at this time the relative error of the atmospheric transmittance of the transmissometer is $n\%$, then the following can be expressed:

$$P_r(n) = \tau_d \cdot P_n(0), \tag{25}$$

$$\frac{\tau_d}{\tau_0} = 1 \pm n\%. \tag{26}$$

Substitute Eqs. (24) and (25) into Eq. (23) to obtain the following:

$$T_0 = (\tau_0 - \tau_d) P(0). \tag{27}$$

Substitute Eqs. (26) into (27) to obtain the following:

$$T_0 = \pm n\% \cdot \tau_0 \cdot P(0). \tag{28}$$

Because $P_r(0)$ is less than $P(0)$, substitute Eq. (28) into Eq. (1) to obtain the following:

$$\frac{P_r(0)}{P(0)} = 1 - n\% \cdot \tau_0. \tag{29}$$

Because the true value of Eq. (29) is 1, when the baseline length is 0 and is similar to Eqs. (15) and (29) then

$$\frac{\Delta P_r(0)}{P_r(0)} - \frac{\Delta P(0)}{P(0)} = n\% \cdot \tau_0. \tag{30}$$

Substitute Eq. (30) into Eq. (22) to obtain

$$\frac{\Delta\tau_d}{\tau_d} - \frac{\Delta\tau(r_n)}{\tau(r_n)} = n\% \cdot \tau_0, \tag{31}$$

where $n\%$ is the relative error of the atmospheric transmittance of the transmissometer as mentioned above. Therefore, the relative error of the atmospheric transmittance of the MVMS can be rewritten from Eq. (31) as follows:

$$\frac{\Delta\tau(r_n)}{\tau(r_n)} = n\% \cdot (1 - \tau_0). \tag{32}$$

B. Relative Error of the MOR

1. Relative Error of the Transmissometer

Similar to Eq. (10), the MOR can be measured by a transmissometer as

$$V = -\frac{3l}{\ln \tau}, \tag{33}$$

where V is the MOR, l is the baseline length of the transmissometer, and τ is the transmittance measured by the transmissometer.

According to the partial derivatives of Eq. (33), regardless of the location error of the transmissometer, the relative error of the MOR measured by a transmissometer can be calculated as follows:

$$\frac{dV}{V} = -\frac{1}{\ln \tau} \cdot \frac{d\tau}{\tau}. \tag{34}$$

2. Relative Error of the MVMS

The MOR system error can be obtained by calculating the partial differential of Eq. (12), as follows:

$$dV = \frac{3 \cdot \left(\sum_{i=1}^{n} r_i^2\right) \cdot \left[\sum_{i=1}^{n} \frac{r_i}{\tau(r_i)} \cdot d\tau(r_i)\right]}{\left[\sum_{i=1}^{n} r_i \cdot \ln \tau(r_i)\right]^2}. \tag{35}$$

Because Eq. (12) can also be rewritten as

$$3 \cdot \sum_{i=1}^{n} r_i^2 = -V \cdot \left[\sum_{i=1}^{n} r_i \cdot \ln \tau(r_i)\right], \tag{36}$$

$$\sum_{i=1}^{n} r_i \cdot \ln \tau(r_i) = -\frac{3 \cdot \sum_{i=1}^{n} r_i^2}{V} \tag{37}$$

substitute Eqs. (36) and (37) into Eq. (35) to obtain the following:

$$\frac{dV}{V} = \frac{V}{3 \cdot \sum_{i=1}^{n} r_i^2} \cdot \left[\sum_{i=1}^{n} r_i \cdot \frac{d\tau(r_i)}{\tau(r_i)}\right]. \tag{38}$$

The results of Eq. (38) can be further calculated using V, r_i, and $\frac{d\tau(r_i)}{\tau(r_i)}$, where the baseline lengths r_i of MVMS are 5 m, 10 m, 15 m, 20 m, 25 m, 30 m, 35 m, 40 m, 45 m, and 50 m, and $\frac{d\tau(r_i)}{\tau(r_i)}$, as shown by Eq. (32).

4. EXPERIMENTAL SETUP

The MVMS consists of a laser transmitter and receiver. An MSL-FN-532 (CNILASER, ChangChun, China) with a wavelength of 532 nm was used as the laser source and was fixed inside the transmitter. A THORLABS DET100A was used as the photoelectric detector. A photoelectric detector and an industrial computer were included on the platform to measure the extinction coefficient. The structure of the MVMS is depicted in Fig. 4. The system hardware parameters are listed in Table 1.

The receiver moved from 0 m to 55 m at a speed of 0.3 m/s, stopping every 5 m and remaining motionless for 3 s to measure and record the data. The extinction coefficient and

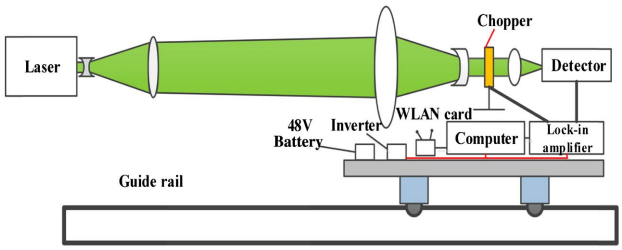

Fig. 4. Diagram of the MVMS.

Table 1. MVMS Hardware Parameters

Major Components	Parameters	
Laser	Wavelength	532 ± 1 nm
	Beam divergence	<1.2 mrad
	Power stability	<1%
	Beam diameter	~2 mm
Chopper	Chopping frequency	20–1 kHz
	Leaf blade groove angle	18°
	Data bits	8
Lock-in amplifier	Full range sensitivity	1 nV–1 V
	Input signal frequency range	1 mHz–100 kHz
Photoelectric detector	Wavelength coverage	350–1100 nm
	Output voltage	0–10 V

visibility were calculated after the receiver moved to 55 m and back twice. Thus, the system obtained four measured values at every measurement point. The mean value of the four measured values was used to calculate the extinction coefficient.

To shorten the experimental cycle, a stalinite atmospheric environment simulation chamber (AESC) was constructed outside the MVMS to simulate a low-visibility environment for several hours. An external photo of the AESC is shown in Fig. 5. A photograph showing the interior of the AESC is presented in Fig. 6.

Fig. 5. Photograph of the exterior of the AESC.

Fig. 6. Photograph of the interior of the AESC.

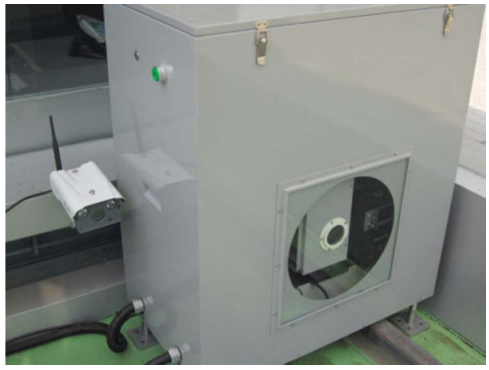

Fig. 7. Transmitter and receiver of the MVMS.

The transmitter and receiver of the MVMS are shown in Fig. 7.

5. CALCULATION AND DISCUSSION

The true value of the transmittance can be calculated using Eq. (34) if the MOR and baseline length are known. Figure 8 shows the true values of the atmospheric transmittance for different given MOR values and baseline lengths.

Figure 8 shows that for the same MOR, as the baseline length decreases, the true value of the transmittance increases.

The relative errors of the MOR measured by the transmissometer for different given baseline lengths and MOR values and a relative error of the transmittance of 1% can be calculated using Eq. (35) and are shown in Fig. 9.

According to Fig. 9, the relative error of the MOR measured by the transmissometer decreases as the MOR decreases. Additionally, as the baseline length of the transmissometer increases, the relative error of the MOR decreases. A 1% relative error in the transmittance measured by the transmissometer with a baseline length of 5 m can cause up to 666.67% relative error in the MOR.

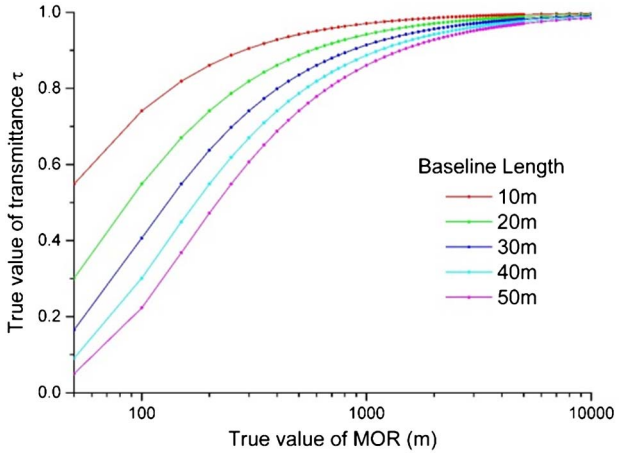

Fig. 8. True values of the transmittance for different given MOR values and baseline lengths.

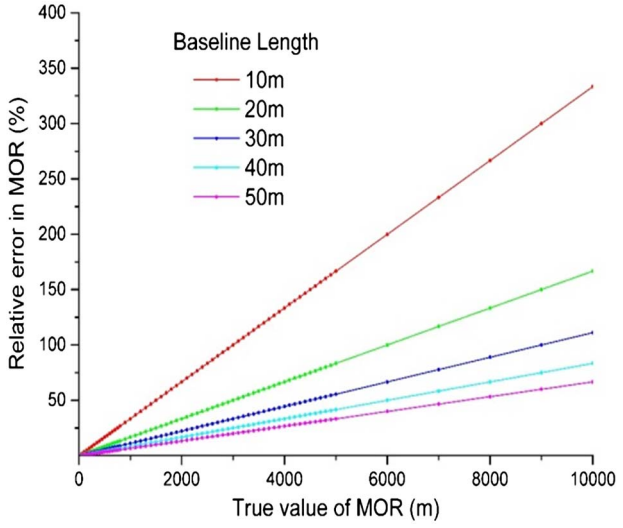

Fig. 9. Relative error of the MOR measured by the transmissometer for different baseline lengths and MOR values.

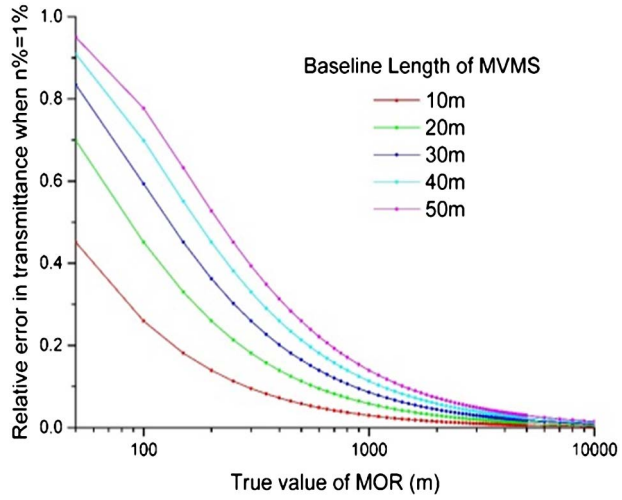

Fig. 10. Relative error of the transmittance of the MVMS when $n\% = 1\%$.

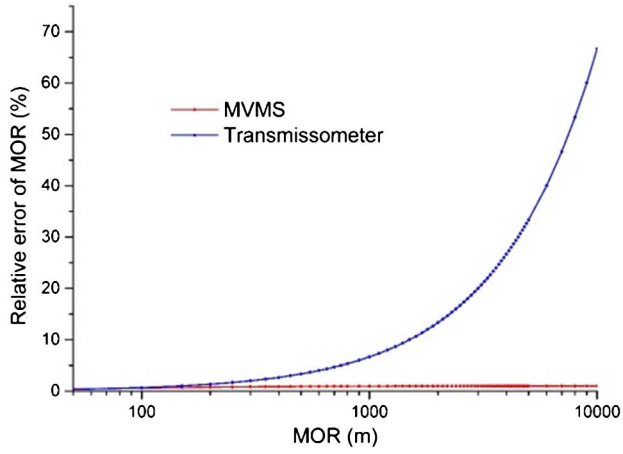

Fig. 11. Comparison of the relative error of the MOR.

Figure 10 presents the relative error of the transmittance determined using the MVMS to measure the MOR with a hardware similar to that of the transmissometer and a relative error of the transmittance of 1%.

Figure 10 shows that the relative error in transmittance is substantially reduced using the MVM. However, the reduction of the relative error was not constant for different given true values of the MOR: As the MOR increased, the reduction increased, and as the baseline length decreased, the relative error of the transmittance also decreased.

The relative errors of the MOR for the MVMS and the transmissometer with a baseline length of 50 m are compared in Fig. 11.

Figure 11 demonstrates that the relative error of the MOR measured by the MVMS is substantially smaller than that of the transmissometer, especially for high MOR values. The relative errors of the MOR measured by the MVMS and transmissometer under various typical MOR conditions are listed in Table 2.

Because the relative errors of the transmittance measured by different hardware systems may not be comparable, to verify the accuracy of the MVM, the measurement results were collected and processed using a method similar to that of the transmissometer with a fixed distance between the transmitter and receiver. These data and those obtained by the MVM were compared. Experiments were performed in the AESC to simulated a change in visibility from high to low and low to high. Both methods were used to process the experimental data, and the results are shown in Figs. 12 and 13.

Figures 12 and 13 demonstrates that under all types of visibility conditions, the results from the transmissometer can be corrected by the MVMS. The error bars in Figs. 12 and 13 represent 5%. Under higher-visibility conditions, the MVMS can reduce the measurement errors to a lesser degree than under lower-visibility conditions. The lowest error reduction was 1.105%, which was obtained when the visibility was

Table 2. Relative Errors of MOR Measured by the MVMS and Transmissometer

MOR (m)	50	100	200	300	400	500	600	700	800	900	1000
Relative error of transmissometer (%)	0.33	0.67	1.33	2	2.67	3.33	4	4.67	5.33	6	6.67
Relative error of MVMS (%)	0.40	0.59	0.76	0.83	0.87	0.89	0.91	0.92	0.93	0.94	0.94
MOR (m)	1100	1200	1300	1400	1500	1600	1700	1800	1900	2000	2500
Relative error of transmissometer (%)	7.33	8	8.67	9.33	10	10.67	11.33	12	12.67	13.33	16.67
Relative error of MVMS (%)	0.95	0.95	0.96	0.96	0.96	0.96	0.97	0.97	0.97	0.97	0.98
MOR (m)	3000	3500	4000	4500	5000	6000	9000	10000			
Relative error of transmissometer (%)	20	23.33	26.67	30	33.33	40	60	66.67			
Relative error of MVMS (%)	0.98	0.98	0.98	0.99	0.99	0.99	0.99	0.99			

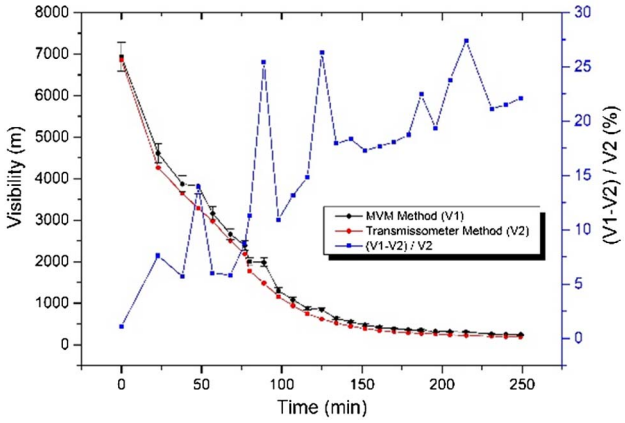

Fig. 12. Comparison of the performance of the MVM and the transmissometer method (visibility change from high to low).

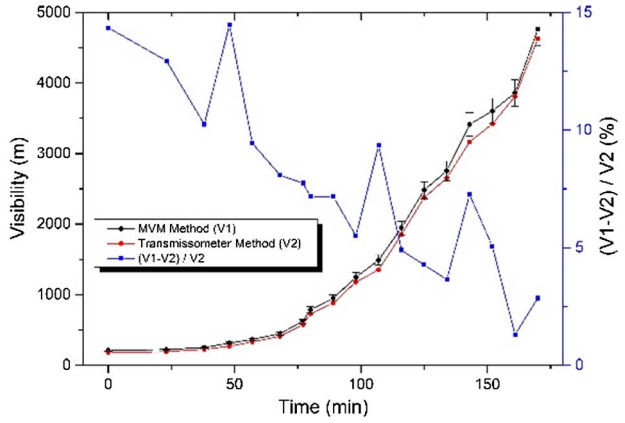

Fig. 13. Comparison of the performance of the MVM and the transmissometer method (visibility change from low to high).

6933.42 m. The highest error reduction achieved was 27.42%, which was obtained at a visibility of 308.47 m.

6. CONCLUSION

This paper proposes a new method for measuring atmospheric transmittance and for calculating the extinction coefficient and MOR. An experiment demonstrating its practical application is also reported. Error analysis revealed that the relative error of the atmospheric transmittance using the MVM is $1 - \tau_0$ times that of the atmospheric transmittance measured using the transmissometer. The results obtained assuming a 1% relative error in the atmospheric transmittance measured by the transmissometer are also reported. Furthermore, experimental data were collected using the MVMS and processed by both methods. This work demonstrated that the proposed system can improve the measurement accuracy under all types of visibility conditions. The lowest error reduction was 1.105%, which was obtained at a visibility of 6933.42 m. The highest error reduction was 27.42% and was achieved at a visibility of 308.47 m. The measurement results of the MVMS can be used as standard values for the calibration of visibility sensors.

Funding. National Natural Science Foundation of China (NSFC) (41174130, 41227804, U1433202, U1533113); Applied Basic Research Programs of Science and Technology Department of Sichuan Province (2015JY0109); Starting Foundation of Civil Aviation University of China (CAUC) (2016QD05X).

REFERENCES

1. J. Wang, X. Liu, X. Yang, M. Lei, S. Ruan, K. Nie, Y. Miao, and J. Liu, "Development and evaluation of a new digital photography visiometer system for automated visibility observation," Atmos. Environ. **87**, 19–25 (2014).
2. J. L. Wang, Y. H. Zhang, M. Shao, X. L. Liu, L. M. Zeng, C. L. Cheng, and X. F. Xu, "Quantitative relationship between visibility and mass concentration of PM2.5 in Beijing," J. Environ. Sci. **18**, 475–481 (2006).
3. J. F. Leys, S. K. Heidenreich, C. L. Strong, G. H. McTainsh, and S. Quigley, "PM_{10} concentrations and mass transport during "Red Dawn"—Sydney 23 September 2009," Aeolian Res. **3**, 327–342 (2011).
4. T. Czarnecki, K. Perlicki, and G. Wilczewski, "Atmospheric visibility sensor based on backscattering using correlation coding method," Opt. Quantum Electron. **47**, 771–778 (2015).
5. World Meteorological Organization, *Guide to Meteorological Instruments and Methods of Observation* (Secretariat of the World Meteorological Organization, 2008).
6. S. Engel and K. Heyn, "Measurement of atmospheric transmission and determination of visual range," UK patent 2410795A (August 10, 2005).
7. D. T. Wayne and C. N. Reinhardt, "Atmospheric transmissometer using a modulated optical source," U.S. patent US9,236,939 (December 10, 2015).
8. K. Mohan, A. A. Paligan, G. Sivakumar, R. Krishnamurthy, V. Shubha, U. Shinde, R. Mali, and M. Bhatnagar, "Performance study of Drishti transmissometer at CAT III B airport," Mausam **66**, 713–718 (2015).
9. P. M. S. Chandran, C. P. Krishnakumar, W. Yuen, M. J. Rood, and R. Varma, "An open-path laser transmissometer for atmospheric extinction measurements," in *International Conference on Light Optics:*

Phenomena, Materials, Devices, and Characterization (Optics, 2011), pp. 288–290.
10. T. A. Kaurila, "A new instrument for measuring optical transmission in the atmosphere," Proc. SPIE **6543**, 654308 (2007).
11. R. Barrales-Guadarrama, A. Mocholí-Salcedo, M. E. Rodríguez-Rodríguez, V. R. Barrales-Guadarrama, and E. R. Vázquez-Cerón, "A new forward-scatter visibility sensor based on a universal frequency-to-digital converter," Instrum. Sci. Technol. **41**, 445–462 (2013).
12. T. Kähkönen, V. Oyj, and J. Ojanperä, "New forward scatter visibility sensor with unique window contamination compensation method," in *18th International Conference on IIPS* (2002).
13. R. Siikamaki, "New product family of present weather detectors and visibility sensors," Vaisala News **164**(01), 32–33 (2004).
14. F. Tang, S. Ma, L. Yang, C. Du, and Y. Tang, "A new visibility measurement system based on a black target and a comparative trial with visibility instruments," Atmos. Environ. **143**, 229–236 (2016).
15. F. M. Caimi, D. M. Kocak, and J. Justak, "Remote visibility measurement technique using object plane data from digital image sensors," in *IEEE International Geoscience and Remote Sensing Symposium* (IEEE, 2004), pp. 3288–3291.
16. R. Babari, N. Hautière, E. Dumont, J. P. Papelard, and N. Paparoditis, "Computer vision for the remote sensing of atmospheric visibility," in *Proceedings of 2011 IEEE International Conference on Computer Vision Workshops (ICCV Workshops)* (IEEE, 2011), pp. 219–226.
17. F. Taillade, E. Belin, and E. Dumont, "An analytical model for backscattered luminance in fog: comparisons with Monte Carlo computations and experimental results," Meas. Sci. Technol. **19**, 055302 (2008).
18. D. J. Griggs, D. Jones, M. Ouldridge, and W. Sparks, "The first WMO intercomparison of visibility measurements: final report," Instruments and Observing Methods Report No. 41 (World Meteorological Organization, 1990).
19. S. Waas, "Field test of forward scatter visibility sensors at German airports," in *WMO Technical Conference on Instruments and Methods of Observation (TECO-2006)*, St. Petersburg, Russian Federation, 2008, pp. 1–17.
20. H. I. Bloemink, "KNMI visibility standard for calibration of scatterometers," in *WMO Technical Conference on Instruments and Methods of Observation (TECO-2006)*, St. Petersburg, Russian Federation, 2006, pp. 4–6.
21. P. W. Chan, "A test of visibility sensors at Hong Kong international airport," Weather **71**, 241–246 (2016).
22. B. Stephen, M. Michael, S. Thomas, B. David, and G. Hoseph, "Federal aviation administration requirements for runway visual range (RVR) visibility and ambient light sensors," in *11th Conference on Aviation, Range, and Aerospace*, Hyannis, America, 2004, pp. 1–5.
23. J. D. Crosby, "Visibility sensor accuracy: what's realistic," in *12th Symposium on Meteorological Observations and Instrumentation* (AMS, 2003), pp. 1–5